

Mechanical Performance of Novel Split Precast Cap Beams

Zhanke Wu¹ and Jingyu Qiao^{2,*}

¹ Shanghai Municipal Engineering Design Institute (Group) Co., Ltd., Shanghai 200092, China;

² Tongji Architectural Design (Group) Co., Ltd., Shanghai 200092, China.

* Correspondence: sz22qjy@tjad.cn

Abstract: In this study, an innovative split precast assembly technique for bridge cap beams is proposed, and its structural performance is investigated via experimental testing and finite element analysis. A scaled (1:3.6) sample was tested to evaluate the flexural behavior, crack resistance, and ultimate capacity of the split precast cap beam. The results indicate that the proposed technique achieves moderately reinforced flexural failure at cantilever roots with satisfactory ductility, with average crack resistance and safety reserve coefficients of 1.15 and 1.74, respectively. Strain analysis confirmed effective composite action between the precast components and the postcast strip, validating the space plane-section assumption. The experiment reveals localized stress concentrations at the beam ends and cantilever roots that require special reinforcement detailing. A nonlinear finite element model was developed and validated against test data, which showed good agreement and successfully captured behavior, including crack initiation and failure modes. The split precast technique has been successfully implemented in approximately 40 cap beams for the Outer Ring East Section traffic improvement project in Shanghai, China. The findings provide both theoretical and practical foundations for optimizing and promoting this efficient construction method in bridge engineering applications.

Keywords: split precast cap beam; experimental study; finite element analysis; structural performance; bridge engineering

Citation: Wu, Z.; Qiao, J. Mechanical Performance of Novel Split Precast Cap Beams. *Prestress Technology* 2025, 2, 01-15. <https://doi.org/10.59238/j.pt.2025.02.001>

Received: 13/06/2025

Accepted: 24/06/2025

Published: 30/06/2025

Publisher's Note: Prestress technology stays neutral with regard to jurisdictional claims in published maps and institutional affiliations.



Copyright: © 2025 by the authors. Submitted for possible open access publication under the terms and conditions of the Creative Commons Attribution (CC BY) license (<https://creativecommons.org/licenses/by/4.0/>).

1 Introduction

Precast concrete technology has gained widespread attention in bridge engineering because of its advantages in terms of quality control, construction efficiency, and environmental impact reduction [1-3]. Among critical bridge components, cap beams play a pivotal role in transferring superstructure loads to substructures, making their prefabrication methods particularly consequential for project timelines and costs [4-9].

Current lightweight approaches for precast cap beams primarily involve segmental construction methods. However, these methods impose high requirements on match-casting precision, onsite assembly accuracy, and heavy equipment [10-14]. In this study, a novel split precast assembly technique for cap beams, in which the beam is prefabricated as two longitudinal segments along its axis, reducing one component weight by more than 50%, is proposed. Crucially, the split assembly allows immediate structural system formation during erection, eliminating the need for match-casting or temporary supports, thereby reducing costs and construction complexity.

In this method, the cap beam is split into two precast segments along its longitudinal axis, with a reserved postcast strip at the center (Figure 1). One segment incorporates the bottom slab and end plates, serving as the built-in formwork of the postcast strip. After onsite installation, the two segments are connected by reinforcement, and the postcast concrete is poured to form a monolithic load-bearing system. The advantages of this split precast assembly include the following:

- (1) Weight reduction: Longitudinal splitting reduces transport and lifting weights by more than 50%, accommodating construction conditions for most highway and urban bridge cap beams.
- (2) Process efficiency: Segments can be prefabricated simultaneously and individually without match-casting, simplifying production and increasing cost-effectiveness.
- (3) Formwork-free joint construction: The postcast strip uses the precast segments as inherent formwork, saving time and costs.
- (4) Mitigated thermal cracking: Split casting avoids hydration heat issues associated with mass concrete pouring, improving quality.
- (5) Rapid deployment: The system achieves immediate structural integrity after assembly, requires no temporary supports, and minimizes traffic disruption, offering significant socioeconomic benefits and broad applicability.

To investigate the mechanical performance of this split precast cap beam, particularly its crack resistance and safety, in this study, a scaled static failure test on the Shanghai Outer Ring East Section (Huaxia Middle Road–Longdong Avenue) traffic improvement project is conducted. The test evaluates crack propagation patterns, failure modes, deformation capacity, and ultimate load safety margins, providing technical validation for engineering applications.

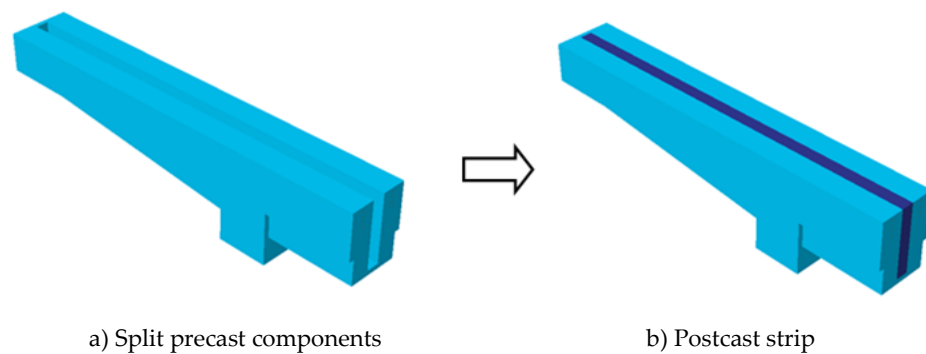


Figure 1 Conception of the split precast cap beam (half structure shown)

2 Experimental Program

2.1 Model Design

The prototype structure was a solid polygonal-section cap beam with a total length of 33.056 m, a height of 3.685 m, and 10.829 m cantilevers on both sides. The beam height varied linearly from 2.9 m at the cantilever root to 1.6 m at the tip, resulting in a total weight of 693.63 tons. Figure 2 shows the elevation of the prototype cap beam.

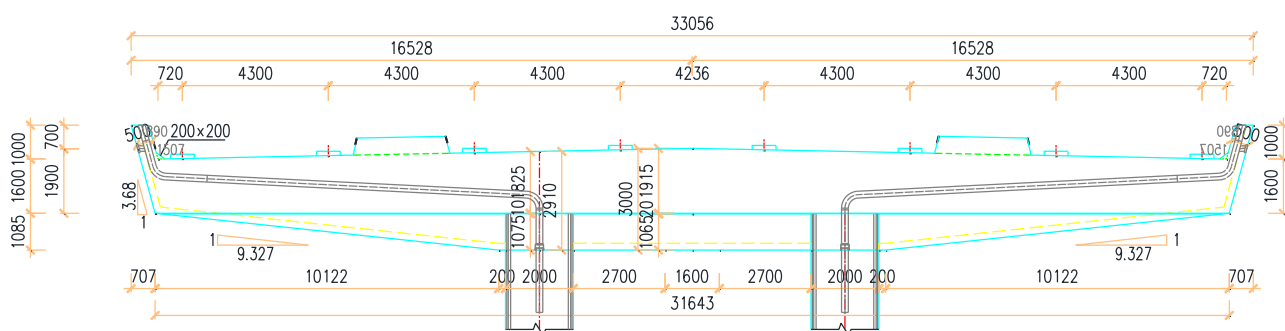


Figure 2 Elevation of the prototype cap beam (unit: mm)

To comprehensively evaluate the structural performance of the split precast cap beam, the focus of this study was the most unfavorable load case at the central pier cap. The loading conditions adhered to China’s “General Specifications for Design of Highway Bridges and Culverts” (JTG D60—2015) [15] and “Specifications for Design of Highway Reinforced Concrete and Prestressed Concrete Bridges and Culverts” (JTG 3362—2018) [16], considering three design combinations: (1) frequent combination for the serviceability limit state (crack resistance), (2) standard combination for the serviceability limit state (deflection), and (3) fundamental combination for the ultimate limit state (safety).

A geometrically scaled model (1:3.6 ratio) was developed to accommodate laboratory constraints while preserving mechanical similitude [17]. The scaled model measured 9.03 m in length, 0.74 m in height, and weighed approximately 13.7 t, with 2.932 m cantilevers exhibiting linear height variation from 0.81 m at the root to 0.44 m at the tip. The scaling methodology ensured strict equivalence in concrete dimensions, reinforcement layouts, including area ratios, and prestressing tendon configurations, while replicating actual construction sequences for split precast assembly. The model consisted of two precast segments (A and B) designed with near symmetry, with the exception that Segment A incorporated the bottom slab and end plates to function as permanent formwork for the postcast strip. Figure 3 shows the dimensions and reinforcement details of the test model.

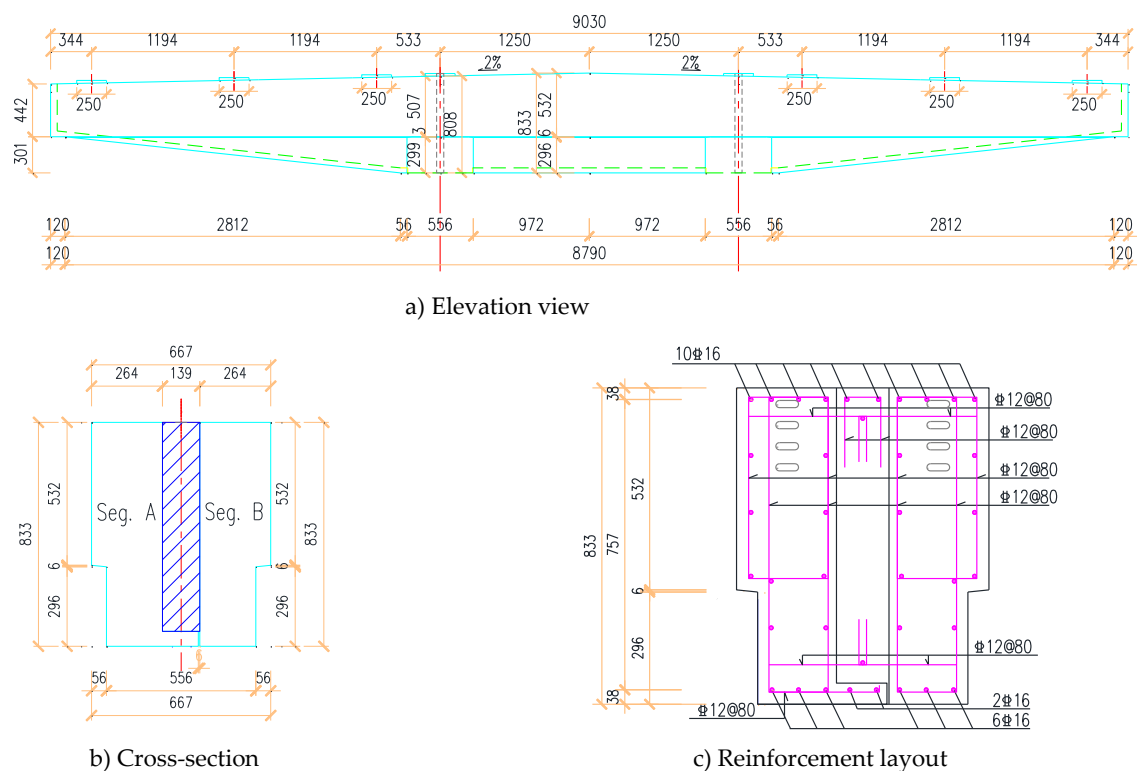


Figure 3 Dimensions and reinforcement details of the test model (unit: mm)

The prestressing system employed post-tensioned 7-wire steel strands with a diameter of 15.24 mm and a tensile strength grade of 1860 MPa, in accordance with the GB/T 5224—2014 standard. The tendon layouts (N1–N4) and their quantities were scaled proportionally based on the original prototype design. Figure 4 shows the prestressing tendon arrangement in the test model. Each of the four tendon profiles comprised two symmetrically arranged bundles, with each bundle containing three strands, achieving a prestressing ratio of 0.65% at the cantilever root. Flat anchors with corrugated metal ducts compliant with GB/T 14370—2015 and JG/T 225—2020 were used for tendon anchorage.

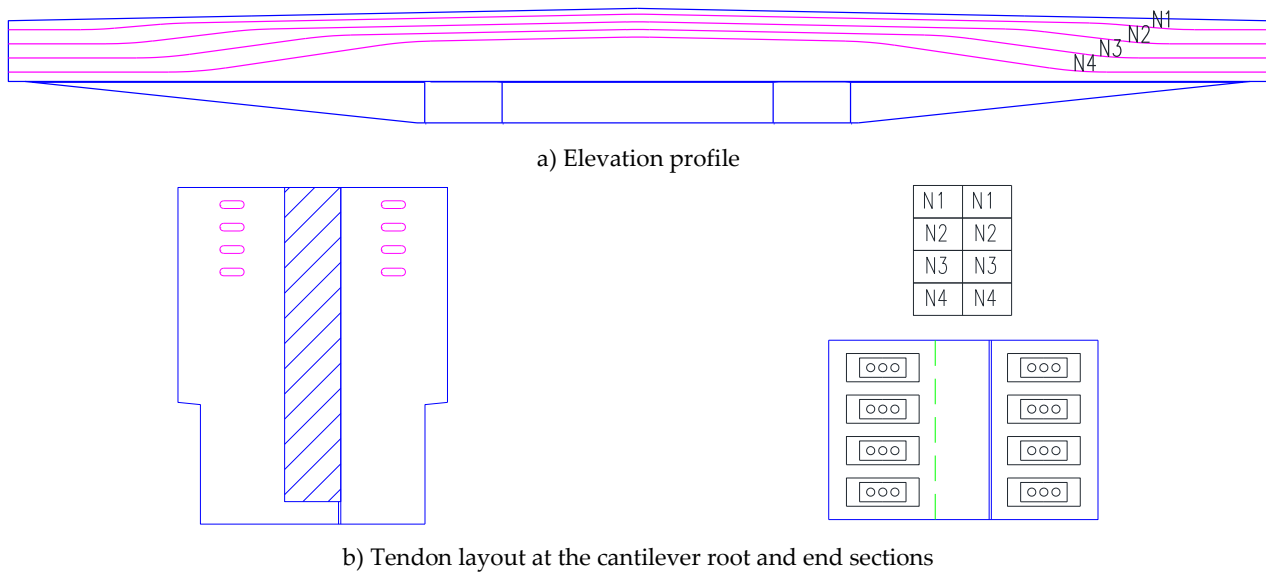


Figure 4 Prestressing tendon arrangement

2.2 Model Fabrication and Assembly

The precast components were manufactured as two separate segments: Segment A, which incorporates the bottom slab, and Segment B. During the fabrication process, PVC (Polyvinyl Chloride) pipes were precisely embedded at the designated column locations and securely fastened to the reinforcement cages. Both segments were cast using C60 concrete, with specified cover thicknesses of 2.0 cm on the exterior surfaces and 1.0 cm on the interface sides, to ensure optimal bonding with the subsequent cast-in-place concrete.

Prior to assembly, the mating surfaces of both precast segments were meticulously roughened by hammering to improve the bond performance between the precast components and the cast-in-place concrete. After concrete curing and 100% design strength, the first-stage prestressing was implemented in the factory, involving the tensioning and grouting of 2 N3 tendon bundles.

The assembly process commenced with the sequential lifting and positioning of Segments A and B. After precise alignment, reinforcement was installed and secured in the joint region. The postcast strip was then filled with concrete, completing the monolithic connection between segments. After the full design strength in the postcast concrete was reached, the second-stage prestressing, which consists of the tensioning and grouting of 2 N2 and 2 N4 tendon bundles, was executed. The fully assembled cap beam was subsequently installed on the test setup (ground anchor beam), where a dead load compensation load was applied before conducting the third-stage prestressing, which involved the tensioning and grouting of the remaining 2 N1 tendon bundles. This phased prestressing sequence ensured proper stress distribution before the test loading program.

2.3 Test Setup

The experimental investigation employed a carefully designed loading and measurement system to accurately evaluate the structural performance of the split precast cap beam. Because the study focused on the cantilever behavior of the cap beam rather than the pier column connection, the grouted sleeve connection of the prototype was simplified using four temporary PSB1080 threaded steel bars (diameter of 40 mm) to simulate the actual connection stiffness. The test specimen was lifted and assembled onto a pier column that had been monolithically cast with the ground anchor foundation, with a 20-tons preload applied to the anchor bars to simulate permanent load effects.

The loading system utilized an efficient anchor reaction system with positioned hydraulic jacks. Two 200-tons capacity hydraulic jacks were installed at locations corresponding to the actual bearing positions, one at the side girder support and another at the nearest intermediate girder support. To ensure stability during asymmetric loading conditions, restraint devices were installed at both the midspan and opposite cantilever ends. Steel-rubber bearing pads were incorporated beneath the jacks to better simulate superstructure load transfer characteristics, adapt to the angular deformation of the beam, and prevent stress concentration at loading points.

The loading protocol was carefully developed to replicate the critical bending moment distribution obtained in the prototype structure, with particular attention to the cantilever root section, which was identified as the key control location. After baseline conditions were established through three cyclic preloading cycles at 20 kN, the test progressed through incremental loading stages. Table 1 shows the loading case for the test model. Each 50 kN load increment was maintained for five minutes to allow for comprehensive crack observation and documentation. After completion of the basic combination loads, the test proceeded to failure by applying continuous loading exclusively at the side support location. The side support was selected as the primary failure loading point because of the heavy traffic considerations.

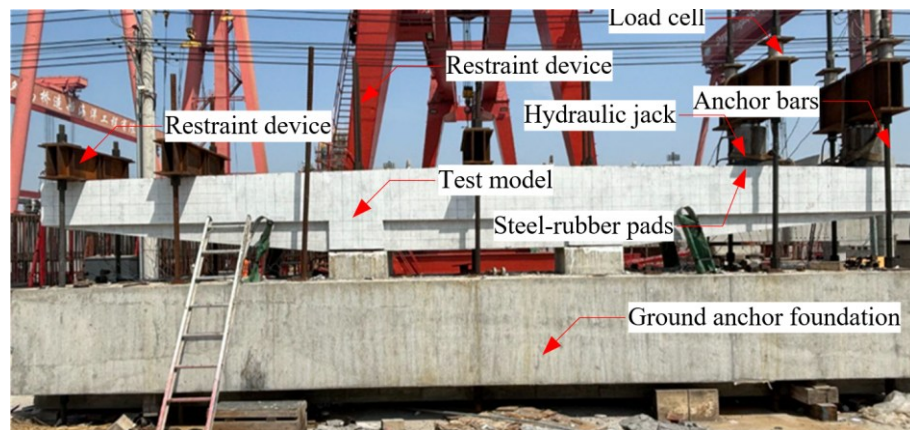


Figure 5 Test setup configuration

Table 1 Loading case for the test model cited

Loading Case	Edge Support Load (kN)	Intermediate Support Load (kN)
Dead load compensation	32.49	32.49
Phase I (precast box girders)	188.35	155.95
Phase II (pavement and overlays)	239.28	206.87
Frequent combination	305.90	273.50
Standard combination	334.46	302.05
Basic combination	420.38	381.49
Ultimate capacity (code value)	1,008.85	381.49

A comprehensive instrumentation scheme was implemented to capture all essential structural responses. The measurement system included 100 tons load cells on each reaction anchor for precise loading monitoring, complemented by an array of strain gauges and displacement transducers. Concrete strain measurements focused on longitudinal strains at top and bottom fibers as well as cross-joint strains, whereas reinforcement strain monitoring main bars in both precast segments and the postcast strip, as well as the connection bars. Displacement measurements employed 15 cm-range wire transducers at critical locations to track global deformation patterns. All the data were collected using a Donghua 3816N static strain testing system with

appropriate strain gauges (120-1AA for steel and 120-80AA for concrete) and Donghua 5G202 wire displacement transducers, ensuring measurement accuracy.

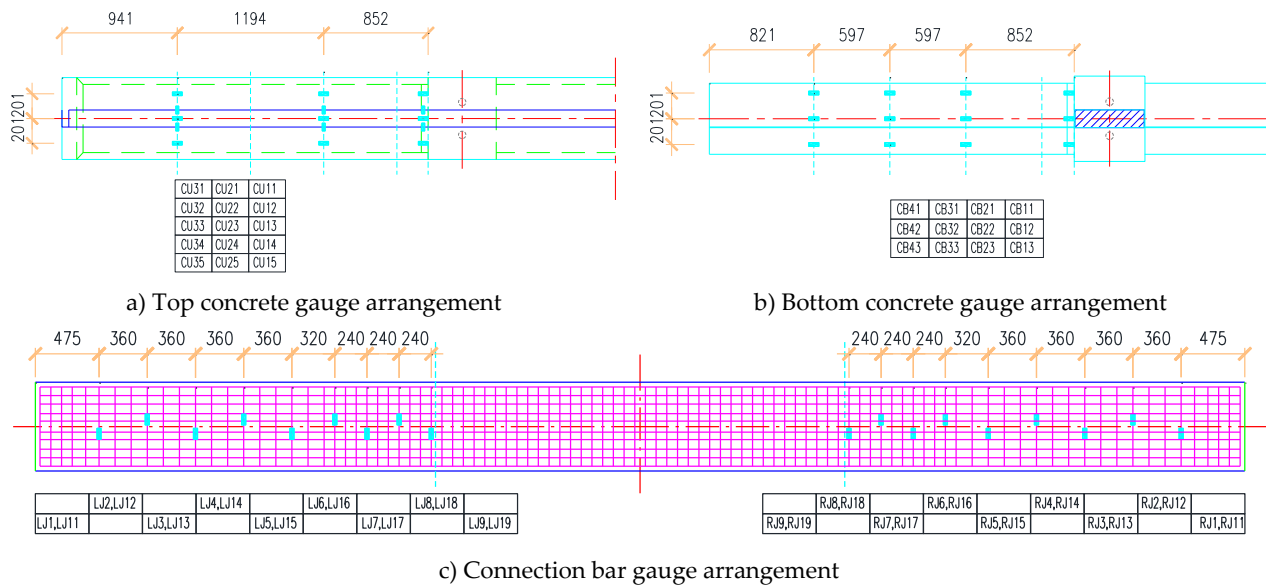


Figure 6 Instrument layout diagram (unit: mm)

3 Experimental Results and Analysis

3.1 Crack Development and Failure Modes

The test beam had similar failure characteristics in both cantilevers under symmetrical loading conditions. When the load was below 69 t, the beam remained in the elastic stage without visible cracks. Initial transverse through-cracks appeared at the top surface of both cantilever roots at 69 t, accompanied by noncontinuous transverse cracks in the midspan postcast strip.

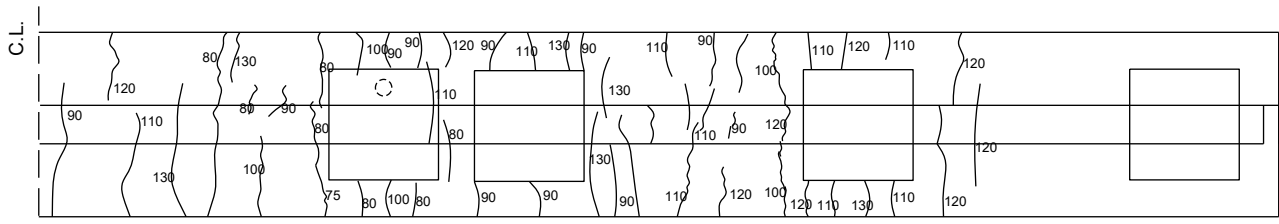
As loading increased, cracks developed systematically. The top surface cracks fully penetrated to form typical vertical flexural cracks that progressively extended downward, with crack widths continuously increasing and new cracks emerging regularly. A uniformly distributed crack pattern with a stable spacing of 10–20 cm eventually formed.

At approximately 110 tons, flexural cracks at cantilever ends transformed into flexural–shear diagonal cracks extending toward the compression zone at cantilever roots. The failure stage (left cantilever at 135 tons and right cantilever at 150 tons) manifested as typical layered crushing failure in the compression zone, concentrated at cantilever roots with distinct layer-by-layer spalling characteristics. The crushed zone measured approximately 35 cm long and 12 cm high in the left cantilever and 40 cm × 8 cm in the right cantilever.

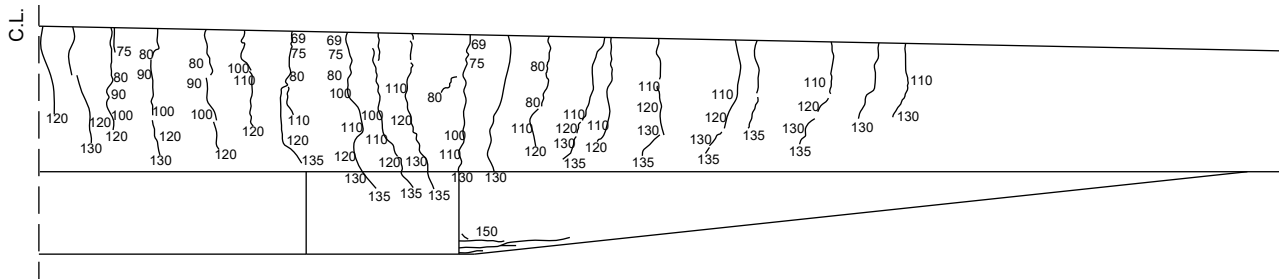
Crack distribution analysis revealed that transverse top cracks were distributed within 3.38 m (left) and 3.42 m (right) from the mid-span. Most cracks exhibited excellent continuity at the postcast and precast interfaces without significant misalignment, confirming effective force transfer across the joints. A posttest examination revealed longitudinal interface cracks at the cantilever ends caused by concentrated forces and an approximately 1 mm vertical through-crack in the end plates, which is a phenomenon that is hidden during testing because of bearing obstructions. The excellent collaborative performance between the postcast strip and the precast components was verified by continuous interface cracks and uniform crack spacing, indicating the reliability of the split precast assembly.

The test beams had identical failure characteristics in both cantilevers, with flexural cracks dominating the damage pattern. The ultimate failure mode was characterized by crushing of the concrete at the cantilever root, accompanied by yielding of both compressive and tensile longitudinal reinforcements. However, the

stirrups did not yield. Owing to the concentrated load at the cantilever end, the top connecting rebars at the cantilever end acted as tension ties under local bearing effects and reached yield. On the basis of the failure characteristics, both cantilevers exhibited moderate reinforcement flexural failure at the root section combined with local transverse tension failure at the cantilever end.



a) Top surface (half structure shown)



b) Side surface (half structure shown)



c) Test picture

Figure 7 Crack distribution of the test model



a) Crushing at the bottom



b) Cracks on the top surface



c) Cantilever end

Figure 8 Crack distribution and failure modes of the test model

3.2 Load–Displacement Curves

The load–displacement curves at the loading points are shown in Figure 9. and characteristics values of test model are shown is Table 2. Both cantilevers exhibited

similar development trends, with the left cantilever test being slightly terminated earlier because of the tilting of the reaction anchor rods. The curves clearly exhibit three characteristic phases: an elastic phase, a crack development phase, and a failure phase.

Prior to cracking, the displacement increased linearly with increasing load, indicating elastic behavior in both cantilevers. The cracking moments were identical for both cantilevers at 1,780.2 kN·m, although the right cantilever had a slightly lower stiffness. The yield moments, defined as the bending moments at which the longitudinal reinforcement first reached its yield strength (determined based on strain gauge data), were 2,244.9 kN·m for the left cantilever and 2,093.6 kN·m for the right cantilever.

Experimental observations revealed that the left cantilever experienced localized concrete crushing at the root section at approximately 135 t (corresponding moment: 3,483 kN·m), with the final monitored failure moment reaching 3,517.2 kN·m. The right cantilever showed crushing behavior at an approximately 150 t load (corresponding moment: 3,870 kN·m), achieving a failure moment of 3,881.8 kN·m. The maximum measured deflections were 57.7 mm (left) and 73.0 mm (right).

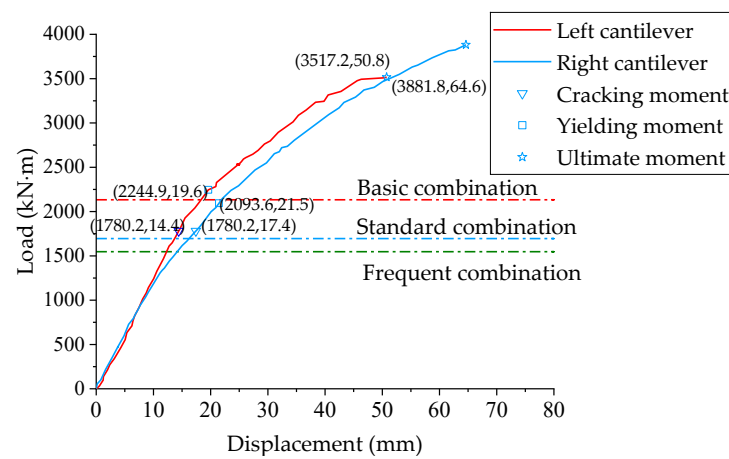


Figure 9 Load–displacement curves

Table 2 Characteristics values of test model

Specimen	Cracking Moment (kN·m)	Yield Moment (kN·m)	Ultimate Moment (kN·m)	Ultimate Deflection (mm)
Left cantilever	1,780.2	2,244.9	3,517.2	57.7
Right cantilever	1,780.2	2,093.6	3,881.8	73.0

3.3 Verification of Crack Resistance and Safety

To facilitate a unified assessment of the crack resistance and safety performance of the prototype structure, the most unfavorable load combination moment at the cantilever root was used as the evaluation criterion. The crack resistance reserve coefficient was defined as the ratio of the cracking load to the frequent combination load, whereas the safety reserve coefficient was defined as the ratio of the ultimate load to the basic combination load. The analysis results are shown in Table 3.

According to the Chinese bridge design code, the material factor for design values is between approximately 1.25 and 1.3. Therefore, the safety factor of the test samples is generally required to be greater than the requirement of the material factor. The test results indicate that the average crack resistance reserve coefficient was 1.15 and that the average safety reserve coefficient was 1.74. These values confirm that the split precast assembled cap beam has sufficient resistance to serviceability limit states (cracking) and ultimate limit states (failure). Future studies could explore the

optimization of reinforcement detailing to further increase crack resistance in high-stress regions.

Table 3 Crack resistance and safety analysis of the cap beam

Specimen	Cracking Moment (kN·m)	Frequent Combination (kN·m)	Ultimate Moment (kN·m)	Basic Combination (kN·m)	Crack Resistance Factor	Safety Reserve Factor
Left cantilever	1,780.2	1,548.0	3,517.2	2,131.6	1.15	1.65
Right cantilever	1,780.2	1,548.0	3,881.8	2,131.6	1.15	1.82

3.4 Concrete Longitudinal Strain

The concrete longitudinal strain behavior of the left cantilever is shown in Figure 10. Prior to cracking, all the sections exhibited a linear elastic strain response, with Section 1 (root section) being the first to crack when the load slightly exceeded the frequent combination level, followed by Section 2 near the basic combination load, whereas Section 3 remained intact until the final failure stage. The cracking tensile strains were measured in the range of 660–710 $\mu\epsilon$ across all instrumented sections.

The post strip developed higher tensile strains than did the adjacent precast concrete at equivalent sections, with the strain increasing progressively from 5 to 60 $\mu\epsilon$ under frequent combination loads to more significant variations at higher load levels. This strain discrepancy was most pronounced at the cantilever root region and gradually stabilized toward the cantilever tip. The strain pattern was directly correlated with the visual crack development sequence, where cracks initiated in the postcast strip before propagating into the precast segments, ultimately forming continuous transverse cracks. This behavior indicates that the prestressing tensioning sequence of the split precast cap beam slightly reduced the tensile stiffness in the postcast region while maintaining effective composite action.

Under ultimate load conditions, the left cantilever reached a maximum compressive strain of -2,488 $\mu\epsilon$ at the root bottom fiber, whereas the right cantilever developed higher strains of -3,117 $\mu\epsilon$. Both values approached the theoretical ultimate compressive strain capacity of the concrete.

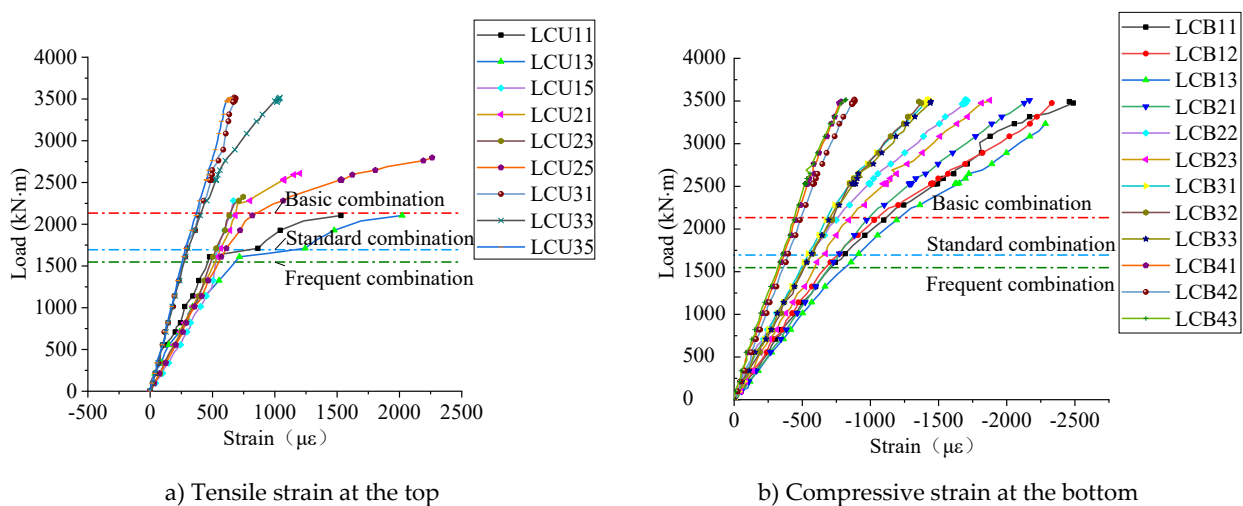


Figure 10 Concrete longitudinal strain (left cantilever)

3.5 Verification of the Plane-Section Assumption

The split precast cap beam components were cast at different times; thus, verification of whether the composite section still satisfies the plane-section assumption was needed. Because the vertical casting was continuous, the vertical

strain distribution can be reasonably assumed to comply with the plane-section assumption. Therefore, analyzing the transverse strain distribution of the composite section was the focus.

Figure 11 shows the transverse distribution of longitudinal reinforcement strain at the top of the critical root section. Under frequent, standard and basic load combinations, the transverse distribution of strain in the top longitudinal reinforcement essentially followed a linear pattern. Linear regression analysis of the strain distributions yielded slopes ranging from 37.1 to 81.9, with coefficients of determination (R2) between 0.03 and 0.21. This finding indicates that the plane-section assumption remains valid for the split precast composite beam. The maintained plane-section behavior validates the design assumption and supports the application of conventional section analysis methods for this split precast cap beam.

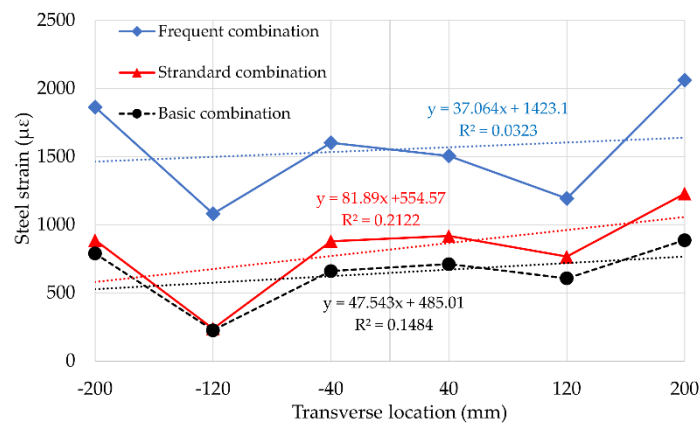


Figure 11 Verification of the plane-section assumption

3.6 Analysis of the Transverse Force Transfer Performance

The strain behavior across the wet joints between the postcast strip and the precast beams was investigated through strain measurements at the beam top (Figure 12). Initially, the interface strains remained relatively small, showing minor compressive strain development under lower load levels. As loading progressed beyond the basic combination, distinct cracking emerged at Sections 1 and 2, whereas Section 3 (located closer to the loading point) maintained predominantly compressive strains due to local stress concentration effects. Under ultimate conditions, the left cantilever exhibited a maximum tensile strain of 406 µε across the joint interface, whereas the right cantilever developed higher strains, reaching 1,950 µε.

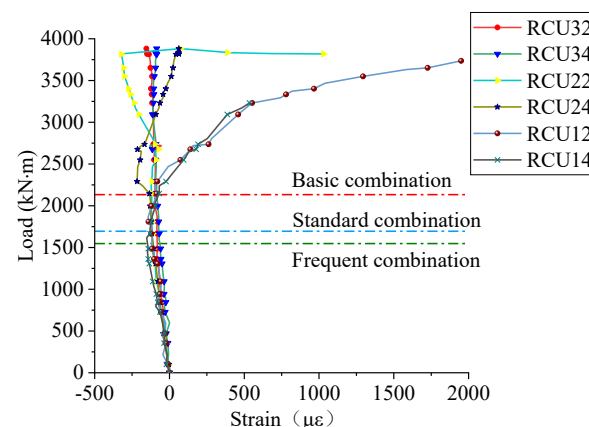


Figure 12 Concrete strain across wet joints (right cantilever)

The top rebars at Section 1 showed substantial strain development, reaching $1,367 \mu\epsilon$ under basic combinations, eventually yielding at failure owing to local bearing effects. The top rebars in Sections 2–9 exhibited minimal strain changes ($<50 \mu\epsilon$) until the advanced loading stages. The bottom rebars displayed a progressive strain increase toward the cantilever root, with maximum strains of $946 \mu\epsilon$ occurring near the root region, which was attributed to Poisson effects in the high compression zone.

The force transfer mechanism evolves progressively with increasing load. At service levels, the system relies primarily on concrete composite action. As loading approaches and exceeds the basic combination, the connection rebars become increasingly engaged, particularly in high-demand regions. These findings validate the effectiveness of the split precast system while identifying specific areas for potential refinement. The cantilever end zones and root regions emerge as critical areas requiring special attention in design.

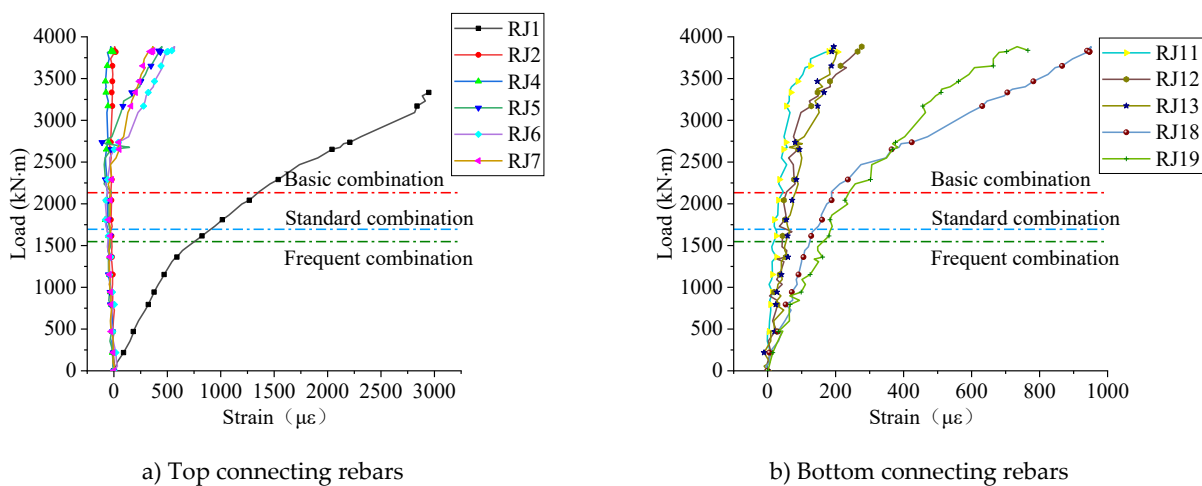


Figure 13 Connecting rebar strain (right cantilever)

4 Finite Element Analysis

A nonlinear finite element model was developed using ABAQUS to conduct a refined numerical simulation of the mechanical behavior of the split precast cap beam [18]. The concrete material was modeled using the Concrete Damage Plasticity (CDP) model, with its constitutive relationship determined according to the Chinese Code for Design of Concrete Structures (GB50010–2010). The material strength parameters were obtained from actual tests on the concrete samples. The model employed a symmetric half-structure approach for computational efficiency, utilizing C3D8R hexahedral reduced-integration elements for concrete and T3D2 truss elements for both reinforcement and prestressing tendons, which were embedded into the concrete using the embedded region method. Tie constraints were applied between the loading supports and the beam top surface. A discretization design balancing computational accuracy and efficiency was used, with a concrete element size of 50 mm and a reinforcement element length of 50 mm.

For the numerical simulation of wet joints in segmental beams, four approaches were considered: cohesive elements, tie constraints, spring elements, and cohesive contact. Considering the highly localized influence of the joint and difficulties in discretizing with solid elements, although tie constraints cannot simulate joint cracking behavior, this study used the cohesive contact model for wet joints. The joint parameters incorporated research findings from this project, including a compressive strength reduction factor of 0.88 and a tensile strength reduction factor of 0.72. Complete bond degradation was assumed at a crack width of 0.2 mm, with the contact state transitioning to “not contacted”.

The finite element model of the cap beam is shown in Figure 14. The analysis included five loading steps: (1) application of first-stage prestress in the precast segment, (2) casting of the postcast strip, (3) tensioning of second- and third-stage prestresses with the application of a superimposed dead load, (4) application of a basic combination load, and (5) application of vertical displacement at the side support. Displacement control was used in the final failure stage to capture post peak behavior. Prestressing forces were applied using the temperature reduction method, with a design tensile control stress of 1,395 MPa and an effective prestress of 1,046 MPa (75% of the design value accounted for 25% of the prestress loss).

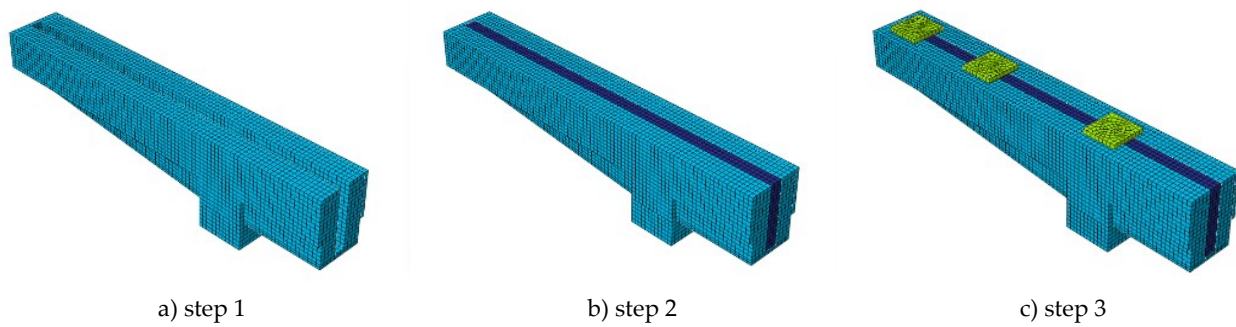


Figure 14 Construction process simulation

Figure 15 compares the numerical and experimental load–displacement curves. Overall, agreement between the FEA and the test results was achieved, with average ratios of the calculated displacement to the tested ultimate displacement and moment being 1.11 and 0.98, respectively. A comparison between the FEM results and the experimental results is provided in Table 4. Compared with the test results, the numerical model results in greater initial elastic stiffness but slightly faster stiffness degradation in the failure stage.

The cracking process in postcast strips and precast segments can be examined through concrete tensile damage. Figure 16 shows the initial characteristics and distribution of concrete tensile damage. Near the basic combination load, cracking first appeared in the postcast strip at cantilever roots with uniform spacing. With increasing load, cracks subsequently developed in the precast segments at the cantilever roots and connected with those in the postcast strip. The cracking load of the postcast strip was approximately 340 kN·m lower than that of the precast segments. The numerical simulation accurately captured the crack initiation sequence and distribution pattern observed in tests, highlighting the need in engineering design to address the earlier cracking behavior of postcast strips by ensuring adequate compressive stress reserves to meet crack resistance requirements.

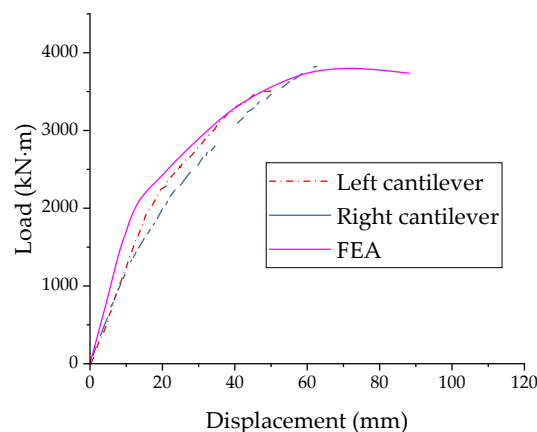


Figure 15 Comparison of load–displacement curves

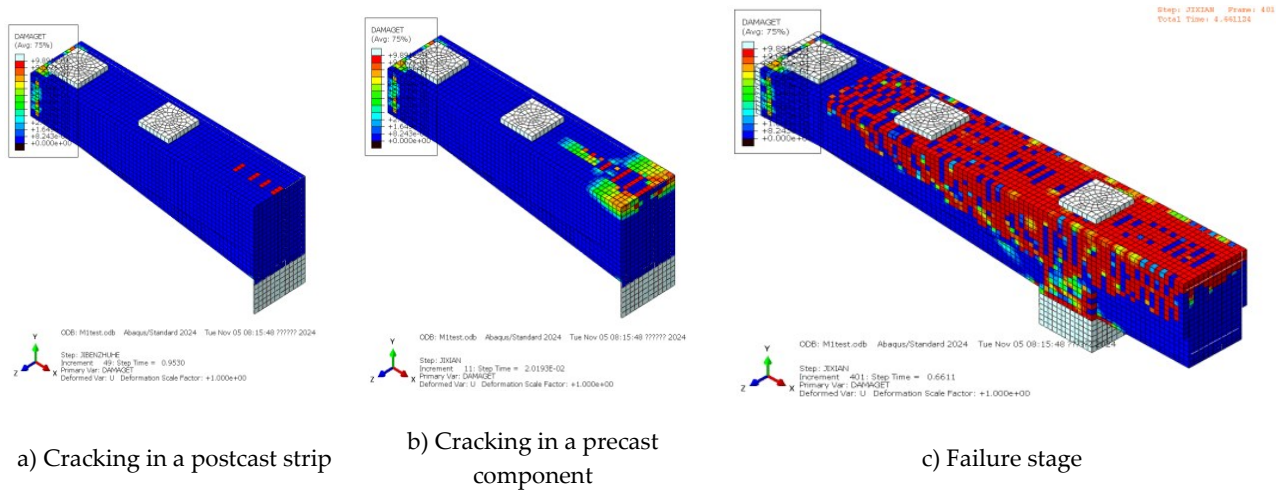


Figure 16 Concrete damage contours

Table 4 Comparison between the FEM results and the experimental results

Parameter	Experimental value	Numerical Value	Ratio (Numerical/Experimental)
Ultimate displacement (mm)	64.6	72.02	1.11
Ultimate moment (kN·m)	3,881.80	3,799.17	0.98

5 Conclusions

In this study, a novel split precast assembly technique for cap beams is proposed, and experimental investigations on a scaled sample are presented. The key findings are as follows:

- (1) The test beam exhibited moderately reinforced flexural failure at the cantilever roots, with both longitudinal reinforcement and prestressing tendons reaching yield at the ultimate state while the compressive concrete was crushed. Stirrups and connecting rebars between segments remained below yield. The splitting technique had minimal effect on the failure mode, although special attention should be given to localized transverse tension failures at the beam ends and cantilever roots.
- (2) The split precast cap beam exhibits reliable crack resistance and a sufficient safety margin, with average reserve coefficients of 1.15 (crack resistance) and 1.74 (safety), meeting engineering requirements.
- (3) As a composite flexural member, while the precast segments showed “stress advancement” in reinforcement, the strain difference between the precast component and the cast-in-place component became insignificant at higher loads. Both the precast and postcast longitudinal reinforcements reached yield at the failure stage.
- (4) The transverse strain distribution follows a linear pattern, confirming the validity of the space plane-section assumption for the composite section.
- (5) Most connecting rebars experienced minimal strain changes (<50 $\mu\epsilon$ under basic combinations), apart from those near loading points affected by local bearing and cantilever roots influenced by D-region effects, where significant transverse tensile strains developed, indicating the need for reinforcement enhancement in these areas.
- (6) The developed finite element model achieved good agreement with the experimental results, successfully capturing key behaviors, including crack initiation sequences and failure modes. The cohesive contact model effectively simulates wet joint behavior, providing a reliable tool for future parametric studies and design optimization.

The proposed technique has been successfully applied to approximately 40 cap beams for the Outer Ring East Section (Huaxia Middle Road–Longdong Avenue) traffic improvement project in Shanghai, China. These split precast cap beams have shown good socioeconomic benefits. Future work should focus on design optimization using finite element methods to facilitate broader application of this technology.

Conflict of interest: All the authors disclosed no relevant relationships.

Data availability statement: The data that support the findings of this study are available from the corresponding author, Qiao, upon reasonable request.

Funding: This research was funded by Shanghai Municipal Transportation Commission Research Project (grant number is JT2024–KY–022). The authors extended their sincere gratitude for the support.

References

1. Akhnoukh, A.K. Accelerated bridge construction projects using high performance concrete. *Case Stud Constr Mat* **2020**, *12*, doi:10.1016/j.cscm.2019.e00313.
2. Saleem, M.A.; Zafar, M.N.; Saleem, M.M.; Xia, J. Recent developments in the prefabricated bridge deck systems. *Case Stud Constr Mat* **2021**, *15*, doi:10.1016/j.cscm.2021.e00750.
3. Zhou, Z.; Zhong, S.; Zhang, J.; Zou, Y.; Liang, H.; Guo, J.; Jiang, J. Discussion on the Development of Bridge Prefabricated Technology and Industrial Manufacturing. *Journal of Chongqing Jiaotong University (Natural Science)* **2021**, *40*, 29-40+72, doi:10.3969/j.issn.1674-0696.2021.10.05.
4. Li, C.; Zhuo, W.; Sun, Z.; Xiao, Z.; Chen, G.; Huang, X. Static Behavior of Segmental Precast Assembled Cap Beam with Corbel Joints. *Journal of Harbin Engineering University* **2023**, *44*, 1328-1335, doi:10.11990/jheu.202112029.
5. Eric E. Matsumoto, M.C.W., Michael E. Kreger, John Vogel, Lloyd Wolf. Development of a Precast Concrete Bent-Cap System. *PCI Journal* **2008**, *53*, 74-99, doi:10.15554/pcij.05012008.74.99.
6. McKee, C.D.; Lee, J.D.; Birely, A.C.; Mander, J.B. Experimental Behavior of Pretensioned Bent Caps with Internal Voids for Weight Reduction. *J Bridge Eng* **2020**, *25*, doi:10.1061/(Asce)Be.1943-5592.0001410.
7. Kim, D.W.; Shim, C.S. Experiments on flexural strength on composite modular bridge pier cap for CFT columns. *Ksce J Civ Eng* **2016**, *20*, 2483-2491, doi:10.1007/s12205-015-1467-9.
8. Hu, F.J.; Yang, C.H.; Zhou, P.M.; Hu, H.; Wang, Y.C. Experimental study on mechanical behavior of precast large-cantilevered UHPC bent caps with π -shaped cross-sections. *Structures* **2024**, *62*, doi:10.1016/j.istruc.2024.106333.
9. Wang, C.; Shen, Y.; Chen, J. Review of research and application of prefabricated and assembled concrete bent caps. *Prestress Technology* **2023**, *1*, 1-14, doi:10.59238/j.pt.2023.03.001.
10. Zhuo, W.; Li, C.; Sun, Z.; Xiao, Z.; Lin, Z.; Huang, X. Experiment on Static Behavior of Segmental Precast PC Cap Beam. *Journal of Tongji University(Natural Science)* **2022**, *50*, 1752-1760, doi:10.11908/j.issn.0253-374x.21376.
11. Li, C.C.; Zhuo, W.D.; Lin, K.Q.; Sun, Y.; Chen, M.Y. Experimental study on flexural behavior of segmental precast large-cantilevered prestressed concrete cap beam. *Structures* **2023**, *57*, doi:10.1016/j.istruc.2023.105166.
12. Lv, W.; Jia, J.; Yao, X.; Zhang, K.; Gu, R.; Lai, M. Experimental study on shear bearing capacity of Ultra - high performance concrete bent cap with thin - walled hollow section. *Structural Concrete* **2025**, doi:10.1002/suco.202400791.
13. Chung, C.H.; Lee, J.H.; Kwon, S.H. Proposal of a New Partially Precast Pier Cap System and Experimental Verification of its Structural Performance. *Ksce J Civ Eng* **2018**, *22*, 2362-2370, doi:10.1007/s12205-017-1268-4.
14. Liu, D.; Wu, J.; Chen, X.; Tian, Y.; Zhang, J. Experimental study and numerical analysis of the flexural performance of key-tooth assembled prestressed concrete cap beam. *Advances in Structural Engineering* **2024**, *27*, 2046-2066, doi:10.1177/13694332241260130.
15. Ministry of Transport of the People's Republic of China JTG D60—2015 General Specifications for Design of Highway Bridges and Culverts. China Communications Press: Beijing, **2015**.
16. Ministry of Transport of the People's Republic of China JTG 3362—2018 Specifications for Design of Highway Reinforced Concrete and Prestressed Concrete Bridges and Culverts. China Communications Press: Beijing, **2018**.
17. Au, A.; Lam, C.; Tharmabala, B. Investigation of prefabricated bridge systems using reduced-scale models. *PCI Journal* **2008**, *53*, 67-95, doi:10.15554/pcij.11012008.67.95.

18. El-Naqeeb, M.H.; Hassanli, R.; Zhuge, Y.; Ma, X.; Bazli, M.; Manalo, A. Cyclic behaviour of GFRP-RC precast column-cap beam frame assembly: A finite element investigation. *Engineering Structures* 2025, 328, doi:10.1016/j.eng-struct.2025.119732.

AUTHOR BIOGRAPHIES

	<p>Zhanke Wu M.E., Senior Engineer, graduated from Tongji University in 2009. Working at Shanghai Municipal Engineering Design Institute (Group) Co., Ltd. Research Direction: Bridge design. Email: 10529020@qq.com</p>		<p>Jingyu Qiao B.E., Senior Engineer, graduated from Tongji University in 1997. Working at Tongji Architectural Design (Group) Co., Ltd. Research Direction: Civil Designer. Email: sz22qjy@tjad.cn</p>
---	---	--	--